Finite element analysis of CFRTP hollow beam under flexural load for an application to vehicle body structure

T. Ohori, T. Matsuo, K. Furukawa and J. Takahashi

Department of Systems Innovation, School of Engineering, The University of Tokyo, Tokyo, Japan

Keywords: *carbon fiber reinforced thermoplastics (CFRTP)), hollow beam*

Abstract

Carbon fiber reinforced thermoplastics (CFRTP) is now in the spotlight because of not only its advantageous properties for mass production automobile but also its ductility. In order to take full advantage of such material properties, the finite element analysis (FEA) is an effective tool. In this study, we developed proper material model of discontinuous CFRTPs for mass production automobile, which are under development and their material model have not been fully understood yet. Experimental and numerical studies for both CFRTP rectangular specimen and several kinds of hollow beams under flexural load were conducted to verify both mechanical properties obtained by small specimen and material model used in FEA.

1. Introduction

In order to achieve reduction of vehicle weight, fiber reinforced composites have been applied to a number of automobile components because of having high-stiffness and high-strength to weight ratio. Especially thermoplastic composites have potential to achieve high-cycle and low-cost manufacturing and high recyclability in contrast to thermosetting composites [1,2]. Above all, polypropylene (PP) has been widely applied to automotive components such as bumper faces and interior parts because of high toughness and simple fabrication techniques [1].

A new type of thermoplastic composite materials, carbon fiber reinforced thermoplastic (CFRTP) which is composed of surface treated carbon fiber (TR50S provided by Mitsubishi Rayon) and maleic-acid modified polypropylene (developed by TOYOBO) [3,4], has been developed for the purpose of applying to automobile frame structures in order to achieve reduction of vehicle weight. In addition, a high-cycle manufacturing technology by compression molding process to make effective use of high formability of the developed CFRTP has also been developed.

In this study, we focus on the finite element analysis (FEA) for the CFRTP hollow beam under flexural load, which can compose at least two types of fiber reinforced configurations. One is a laminated constitution of chopped tapes dispersed at random in in-plane pattern and the other is a unidirectional laminate. We introduce experimental and numerical studies by taking into consideration only chopped tapes CFRTP laminate (CTT laminate) and hybrid composition of unidirectional CFRTP laminate (UD laminate) and CTT laminate.

2 .Material specification

A compression molding of thermoplastic composites is appropriate for high-cycle manufacture [5.6]. Figure.1 shows a molding process from a roll of the prepreg tape with the polypropylene impregnated into a continuous unidirectional bundle of the carbon fibers to a CTT laminate and a specimen. The specimen is cut from a CTT laminate, in which a lot of chopped CF/PP tapes are dispersed at random in in-plane pattern. In this process, the pre-consolidated plate of chopped tapes is heated up to about 210 °C in a infrared heater, and right after that, the heated plate is delivered to and placed on the lower mold set on the press machine, and next, cooled down and compressive pressed around 120 °C with a pressure of 18MPa. Table.1 shows each composition of CTT laminate or UD laminate respectively. From mechanical aspect, the UD laminate has an orthotropic property and the CTT laminate has an in-plane isotropic property.

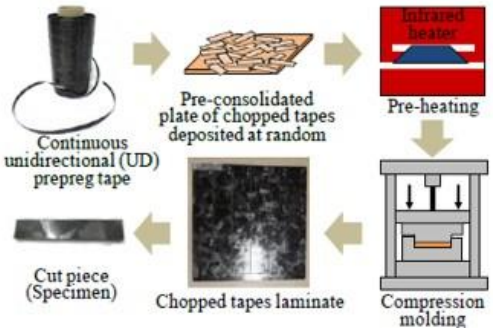

Figure.1. Molding process of CTT laminate.

	CTT laminate	UD laminate
Carbon Fiber	TR50S	TR50S
Volume Fraction	50%	50%
Tape size	Length: 35mm Width: 15mm	(Continuous)
Matrix	Acid modified polypropylene	Acid modified polypropylene
Mechanical property	In-plane isotropic	Orthotropic

Table.1. Composition of CTT and UD laminates.

3. Verification for material model and mechanical parameter

3.1. Bending test

As shown in Figure.2, the strain-stress relationships of CTT laminate and UD laminate were examined by static 3- point-bending test using universal testing machine which can record a load-stroke curve. The test results are shown in Figure.3. Here, for comparison, the graph plots both of strain-stress curves of CTT laminate and UD laminate, whose material main properties are listed in Table.1. From test result, it was found that the flexural fracture behavior of CTT laminate was clearly ductile different from that of UD laminate. That is to say, the CTT laminate stress declines gradually with the strain increasing after the fracture start. In other words, using CTT laminate as a structural material performs a potential of higher fracture-energy-absorbing. On the other hand, the stiffness and strength of CTT laminate are lower than those of UD laminate.

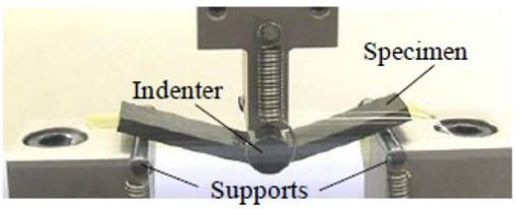

Figure.2. Static 3-point-bending test.

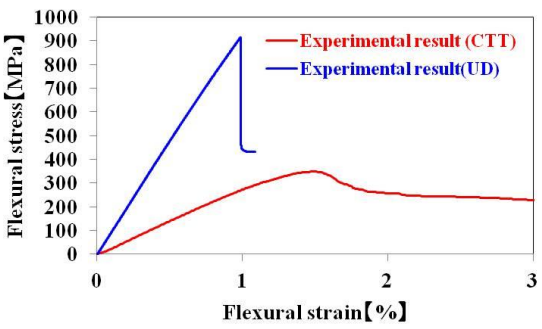

Figure.3. Strain-stress curves of CTT and UD.

3.2. Comparison of experimental result and FEA result

For comparison of experimental result and FEA result, the material model defined in Altair RADIOSS 11.0, MAT25 was used as material property of a laminar ply for the laminated shell element. And, for the pre-processing in Altair RADIOSS 11.0, PROP17 was used as laminated shell element for stacking multi plies defined by MAT25. Based on the rule of mixtures [7], the material properties of CTT laminate and UD laminate assigned to each ply of specimen were defined in MAT25 as indicated Table.2. Each shell element as a ply of CTT laminate has in-plane isotropic property and each shell element as a ply of UD laminate has orthotropic property. And, the failure behavior of all elements was defined to comply with Tsai-Wu yield criteria.

Material property		CTT	UD
Elastic modulus (GPa)	E_1	32	105
	E_2	32	3
	G_{12}	14	1.1
	G_{13}	1	1.1
	G_{23}	1	0.9
Poisson's ratio	ν_{12}	0.3	0.26
	ν_{13}	0.59	0.26
	ν_{23}	0.59	0.59
Strength (MPa)	σ_{1y}	315	1400
	σ_{2y}	315	30
	σ_{1c}	240	400
	σ_{2c}	240	30

Table.2. Material parameters of CTT laminate and UD laminate.

The each experimental result is indicated with the each FEA result in Figure.4. The graphs show the strain-stress relationships calculated from the stroke of the indenter and the vertical load detected by the indenter. As compared to the experimental relationship, it can be said that the FEA material model defined as MAT25 and the mechanical parameters of CTT laminate and UD laminate are almost valid for reproducing the experimental result, especially in the total deformation and the initial fracture point.

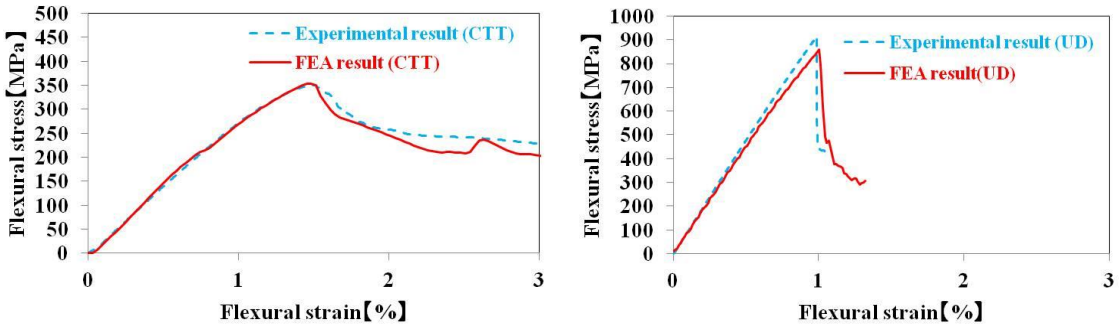

Figure 4. Comparison of experimental result and FEA result (a) CTT laminate (b) UD laminate.

4. Verification for hollow beam-bending

4.1. Bending test

First, for CTT hollow beam, CTT hat-channel beam whose thickness is 2.0mm was

manufactured in the same molding process as Figure.1 shows. And next, a hat-channel beam with the thickness 4.0mm were welded with both a plate as shown in Figure.5 and a hat-channel beam as shown in Figure.6 by a vibration joining method.
As shown in the left and the right of Figure.7, each load-stroke curve of two CTT hollow beams was examined by static 3- point-bending test using universal testing machine. The test results are shown in Figure.8.

Figure.5. Hollow beam (a hat-channel beam and a plate).

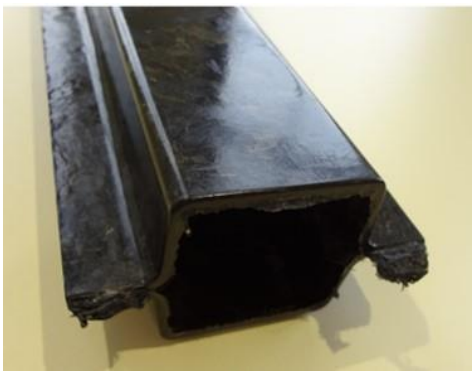

Figure.6. Hollow beam (double hat-channel beams).

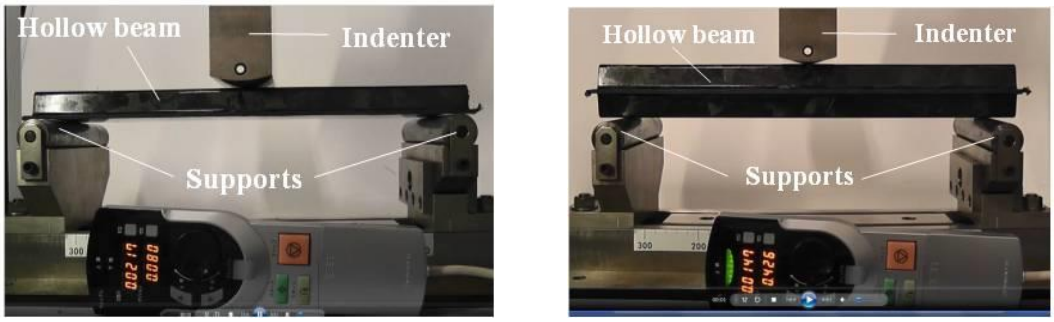

Figure.7. Static 3-point-bending test.

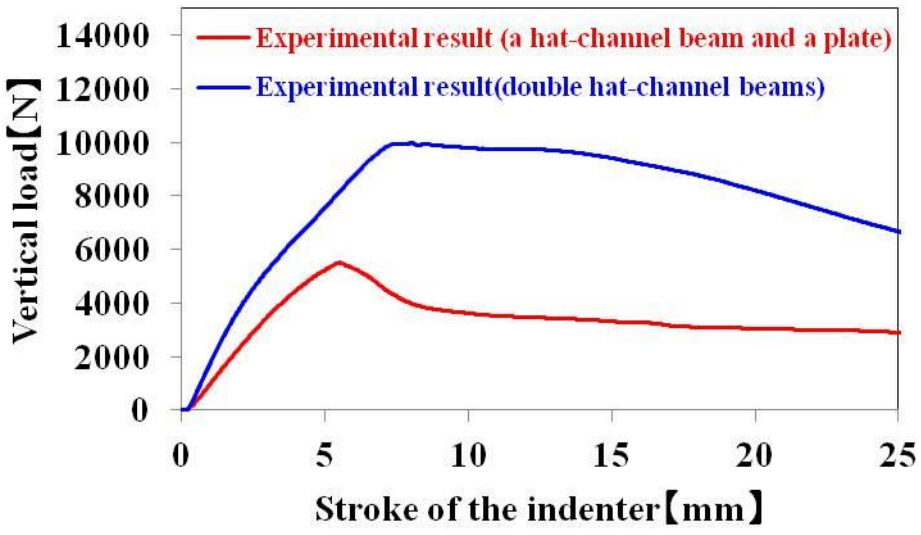

Figure.8. Load-stroke curves of CTT hollow beams.

In the next phase, for the optimized anisotropic CFRTP hybrid hollow beam of CTT and UD, Figure.9 shows the molding process which includes a compression molding with heating and cooling system and a vibration welding. Different from the previous molding process shown in Figure.1, the pre-consolidated CTT sheet and UD sheet were heated up by heat transfer

from the heaters installed in the press machine. Right after reaching up to about 200 °C, the stacked sheets of CTT and UD were cooled down and compressive pressed at a pressure of 10MPa. Through the same process, the stacked hat-section beam of CTT hat-section beam and UD plate were cooled down and compressive pressed. After that, by vibration welding, the hat-section beam and the base plate were combined into a CFRTP hybrid hollow beam as shown in Figure.9.

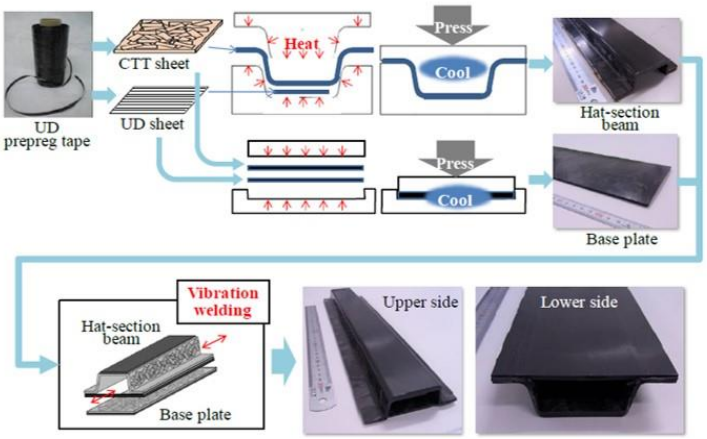

Figure.9. Manufacturing process of anisotropic CFRTP hollow beam.

As shown in Figure.10, the load-stroke curve of hybrid hollow beam was examined by static 3- point-bending test using universal testing machine. The test result is shown in Figures.11 and 12. As Figure.11 shows, the compressive fracture spread from around the corner between the upper UD plate and the side CTT plate.

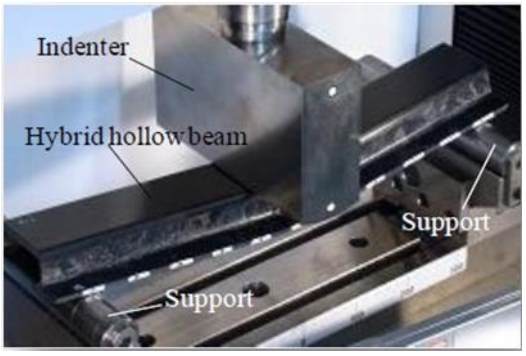

Figure.10. Static 3-point-bending test.

Figure.11. Hollow beam after the 3-point-bending test.

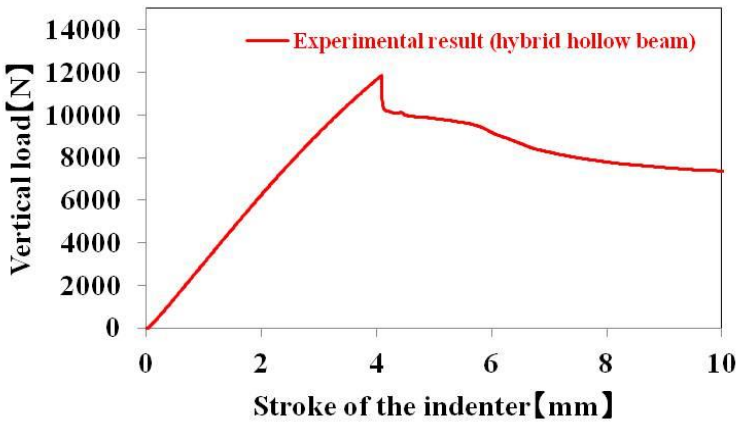

Figure.12. Load-stroke curves of hybrid hollow beam.

4.2. FEA model

The model was designed by using the finite element analytical model which was created in Altair HYPERMESH 11.0. For saving the computational time, 1/4 model was constructed as shown in Figure.13. In this model, the indenter and support had rigid body property. And, the indenter was assigned with a constant speed in the vertical direction and detected the reactive force influenced by the deformation of the hollow beam. Those loading and boundary conditions as well as the meshing properties were imported to Altair RADIOSS 11.0 for an explicit analysis.

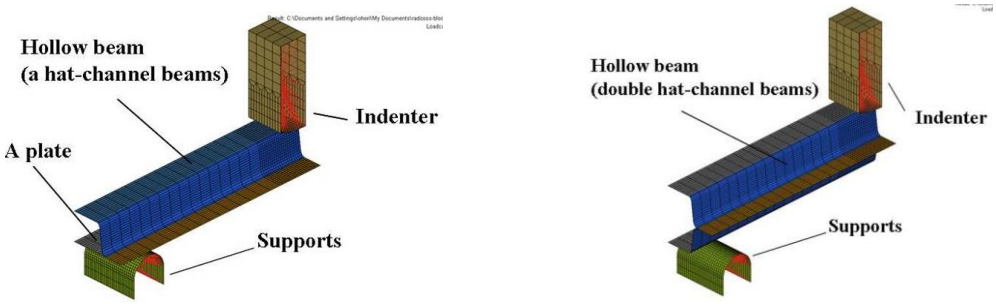

Figure.13. FEA 1/4 model of 3-point-bending test.

4.3. Comparison of experimental result and FEA result

The each experimental result was indicated with the each FEA result in Figures.14-16, the relationship of stroke and load. And the flexural behavior progressing during the test was compared to the post-processing simulation in HYPERVIEW 11.0 for the FEA result. Each comparison represents that the FEA simulation can demonstrate the total deformation of the hollow beam in the experimental behavior.

At the maximum load, the stress distribution in the longitudinal direction of the hollow beam is visualized in a contour figure as shown in Figure.17. The highest compressive stress in all mesh elements appears at the corner section between the upper plate and the side plate with the indenter and the initial fracture starts at the section.

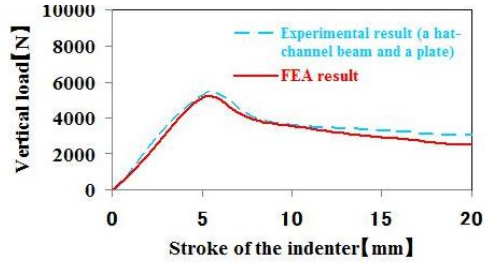

Figure.14. Experimental result and FEA result of CTT hollow beam (a hat-channel beam and a plate).

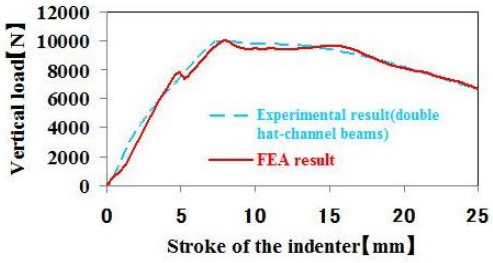

Figure.15. Experimental result and FEA result of CTT hollow beam (double hat-channel beams).

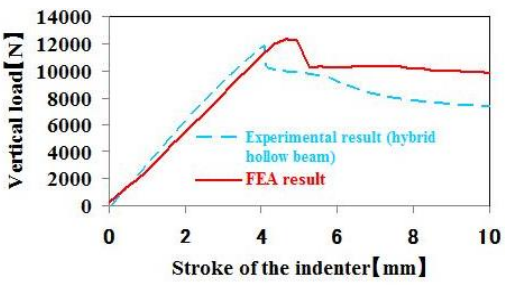

Figure.16. Experimental result and FEA result of hybrid hollow beam.

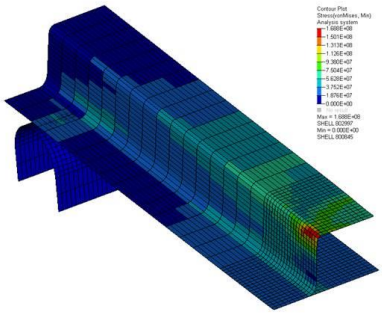

Figure.17. Stress distribution of hollow beam.

5 Conclusions

With first process, the total deformation and the failure behavior of the 3- point-bending test with rectangular specimens of both CTT and UD laminate showed very good agreement with respective FEA results. Hence FEA material model and mechanical parameters were confirmed to be valid.
With second process, experimental results and FEA results for 3- point-bending test of three types of CFRTP hollow beams were compared. All load-stroke relationships including ductile feature after initial fracture showed good agreement, hence we became able to discuss toward an optimal structural design by using this material based on the stress-strain information of FEA.

Acknowledgements
This study was conducted as a part of Japanese METI project "the Future Pioneering Projects / Innovative Structural Materials Project" since 2013fy. Authors would like to express sincerely appreciation to the project members who have provided valuable information and useful discussions. In especially, Toyobo Company provided specimens and deeply committed experiment study.

References

[1] U. K. Vaidya and K. K. Chawla, "Processing of fibre reinforced thermoplastic composites", *International Materials Reviews*, Vol. 53, No. 4, pp. 185-218, 2008.
[2] H. Ning, U. Vaidya, G. M. Janowski and G. Husman, "Design, manufacture and analysis of a thermoplastic composite frame structure for mass transit", *Composite Science and Technology*, Vol. 80, pp. 105-116, 2007.
[3] J. Takahashi, "Strategies and technological challenges for realizing lightweight mass production automobile by using thermoplastic CFRP", *The 12th Japanese-European Symposium on Composite Materials*, Jeju Island, 2011.
[4] T. Hayashi, A. Sasaki, T. Terasawa, and K. Akiyama, "Study on Interfacial Adhesion between Carbon Fiber Thermoplastic Resin and Mechanical Properties of the Composite", *11th Japan International SAMPE Symposium & Exhibition*, Tokyo, 2009.
[5] T. Hayashi and A. Sasaki, "Flexural Behavior of CF/PP hollow beam made by continuous and discontinuous UD tape", *15th European Conference on Composite Material*, Venice, 2012.
[6] M. Ericrson and L. Berglund, "Deformation and fracture of glass-mat-reinforced polypropylene", *Composite Science and Technology*, Vol. 43, pp. 269-281, 1992.
[7] D. Hull and T. W. Clyne, "*An Introduction to Composite Materials"*, 2nd Edition, Press Syndicate of the University of Cambridge, 1996.
[8] T. Matsuo, K. Takayama, J. Takahashi, S. Nagoh, K. Kiriyama and T. Hayashi, "Design and manufacture of anisotropic hollow bean using thermoplastic composite", The 19th international conference on composite materials, 2013.
[9] T. Matsuo, K Kageyama, "New Test Method and Investigation about Unidirectional Compressive Strength for Carbon Fiber Reinforced Thermoplastic Composites", The 38th JAPAN national symposium on composite materials, 2013.